



ORIGINAL RESEARCH ARTICLE

Effect of Cryosoaking Period and Soft-Tempering Temperature on Wear Behavior of AISI H13 Steel

N.B. Dhokey, Tarang Shinde , K.K. Bawane, Akshay Rajankar, and Rajeshwari Mahajan

Submitted: 28 December 2023 / Revised: 14 May 2024 / Accepted: 1 June 2024

Hot work tool steels like AISI H13 are used mainly for high-temperature metal forming operations. The current research includes subjecting AISI H13 tool steel to deep cryogenic treatment and subsequently studying their wear behavior. The specimens were hardened at 1020 °C followed by double tempering at 500 °C for 2 h. The other set of specimens were hardened, double tempered, cryogenically treated (− 185 °C) at different cryosoaking periods. Microstructural analysis and hardness measurements were carried out along with the wear testing on pin-on-disk machine with SAE 52100 counter-face material at room temperature conditions. Double tempering was chosen as a treatment post-hardening. Deep cryogenically treated specimens indicated improved hardness and wear resistance as compared to conventionally treated materials which could be attributed to the precipitation of fine carbides in the matrix of tempered martensite. Minimum wear rate assisted in optimizing soft-tempering temperature at 50 °C post-deep cryogenic treatment.

Keywords AISI H13, carbides, cryogenic treatment, hardness, tempering, wear

1. Introduction

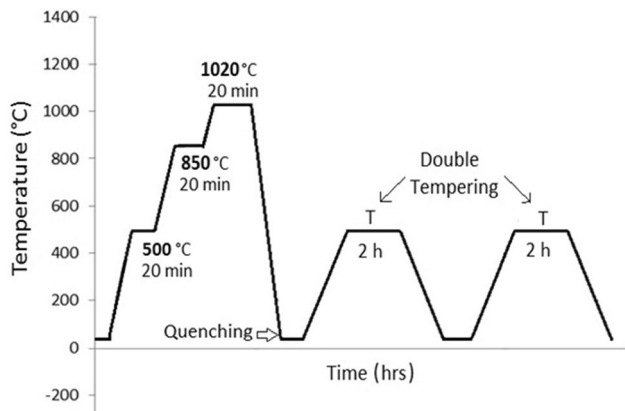
AISI H13 tool steels are used mainly for high-temperature metal forming operations such as hot stamping, piercing, hot forging, hot drawing, hot extrusion, upsetting, swaging and die casting dies of aluminum and copper alloys where operating temperature could reach to 200 °C to around 800 °C. This material needs to possess high strength, high red hardness, wear resistance, toughness, erosion resistance, resistance to softening at elevated temperatures, along with good thermal conductivity and resistance to heat checks (Ref 1-4). AISI H13 includes carbide formers such as chromium (Cr), molybdenum (Mo) and vanadium (V) which form hard, wear resistant as well as high-temperature resistant alloy carbides. The applications such as forming dies include interaction of severe force with the surface. The hardness and wear resistance play a vital role in the life cycle of the forming dies. In order to face such a severe working condition of thermal and mechanical stresses, the material properties need to be upgraded through some treatment. The deep cryogenic treatment (DCT) or cryogenic treatment (CT) has been used by many researchers in order to improve the wear resistance, hardness and fatigue properties of such materials, and the results have been much more encour-

aging (Ref 5-10). Some researchers have performed nitriding on tool steels in order to improve their surface contact resistance, wear resistance especially in the applications like gears, pulleys, shafts, etc. (Ref 11, 12). The cryogenic treatment is accountable for the precipitation of fine tertiary carbide particles in the matrix of tempered martensite (Ref 13-16). Martensitic laths have been found to be sharper, smaller and oriented along specific crystal directions of prior austenite grains within DCT specimens compared to CT specimens (16). The retained austenite also poses a problem in many tool steels after quenching treatment (Ref 17, 18). The cryogenic treatment could be beneficial in the elimination of retained austenite by its conversion into martensite. The cryogenic treatment is a core treatment wherein surface as well as core of the material undergoes microstructural changes which brings about subsequent changes in the material properties. The cryogenic processing has even found applications in biomaterials for their sustainability benefits (Ref 19). Most of the parts undergo failure on account of corrosion when subjected to elevated temperatures as well as corrosive environment. The deep cryogenic treatment has also been effective to enhance the corrosion resistance of tool steels (Ref 20-22). The precipitation of carbides plays an important role in inhibiting the grain growth and also assists in minimization of wear loss (Ref 23). Even some researchers have noted improvement in the tensile strength and elongation in case of cryogenically treated H13 steels (Ref 24). There has been reporting of microvoid formation and decohesion of fine carbide particles in case of H13 steel after cryogenic treatment which has resulted in improvement in the wear and mechanical properties (Ref 25). The refinement of martensite laths has been noted which has resulted in the increase in hardness, strength and other properties (Ref 26). Some researchers have noted marked increase in dimensional stability, fatigue behavior, grindability, hardness, machinability and microstructure of tool steels on account of deep cryogenic treatment (Ref 27-33). DCT facilitates the precipitation of fine and dispersed carbides,

N.B. Dhokey, Department of Metallurgy and Materials Science, COEP Technological University, Pune, India; Tarang Shinde, Department of Mechanical Engineering, Faculty of Engineering, Yashoda Technical Campus, Satara, India; and K.K. Bawane, Akshay Rajankar, and Rajeshwari Mahajan, COEP Technological University, Pune, India. Contact e-mail: tarangshinde@gmail.com.

Table 1 Chemical composition of H13 tool steel (elements in % by weight)

Elements	C	Mn	Si	Cr	Mo	V	Co	S	P	Fe
AISI H13	0.42	0.39	0.98	4.88	1.38	0.86	0.47	0.016	0.022	Balance

**Fig. 1** Processing route for conventionally treated AISI H13 specimens

imparting a robust pinning effect on boundary migration and thereby impeding the initiation and propagation of thermal fatigue cracks (Ref 34). However, care should be taken to avoid grain coarsening which could lead to loss of mechanical properties (Ref 35). Some researchers have substantiated some alternatives such as boron doping in the different steel compositions in order to improve the wear resistance of the material (Ref 36-38).

The retained austenite raises an issue in case of many tool steels like AIS H13, since it decreases the hardness of the material and also get converted to bainite on heating. The present work elaborates the application of cryogenic treatment on AISI H13 tool steels in order to identify its influence on the hardness and wear performance. Soft-tempering temperature has also been standardized since these materials need to undergo mechanical working operations which demand a better combination of mechanical properties.

2. Materials and Methods

2.1 Material and Specimen Preparation

AISI H13 steel material was procured and tested for the chemical composition using vacuum emission spectrometer (Table 1).

The specimens were prepared for wear testing with diameter 8 mm and height 10 mm for AISI H13 tool steel. For hardness testing, the diameter of AISI H13 sample was 20 mm and 20 mm length (height). The diameter to height ratio was maintained properly to get accuracy in the measurements.

2.2 Material Processing

2.2.1 Hardening and Tempering. The specimens were hardened in a furnace (Make: Therlek, 3.8 KW, 230 V, max. operating temperature 1600 °C) at 1020 °C for 20 min. The specimens were covered with activated charcoal to avoid decarburization. Multistage heating was carried out to avoid generation of thermal stresses during heating and for homogenization of temperature along the cross section of sample. The specimens were quenched in rigorously stirred quenching oil. Tempering treatment was carried out in a muffle furnace at a standardized temperature with a heating rate of 7 °C per minute (Fig. 1).

2.2.2 Cryogenic Treatment. The deep cryogenic treatment or cryogenic treatment was performed in a cryobath or cryogenic chamber (Make: Sanmar, Navi Mumbai) at -185°C , at a cooling rate of 3 °C/min by supplying calculated volume of gasified liquid nitrogen through solenoid valve. The cryosoaking period was varied from 8 to 32 h. After completion of regular intervals of cryosoaking period, the specimens were removed from the cryogenic chamber and transferred to an insulated box till the specimens attained the room temperature. Figure 2(a) shows processing route for specimens undergoing cryogenic treatment and soft tempering.

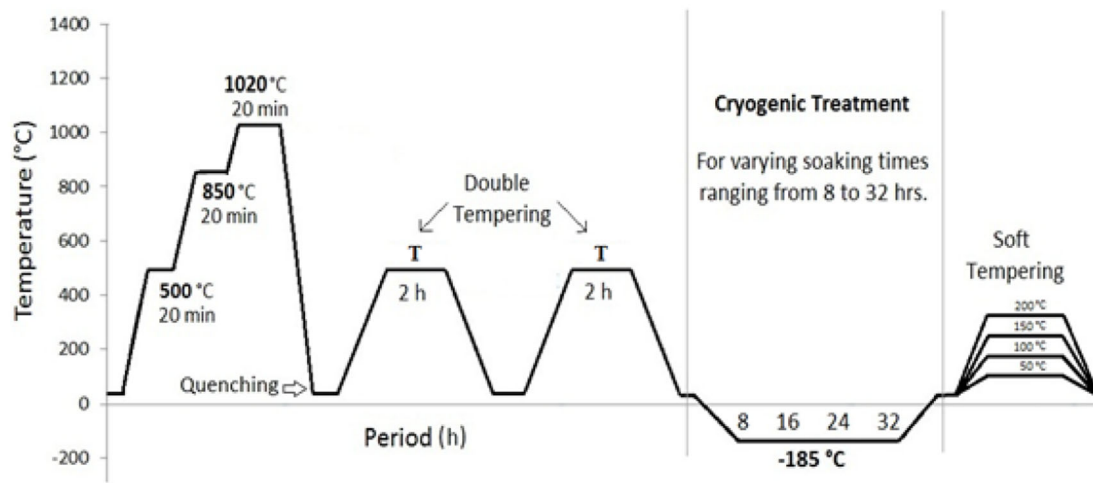
2.2.3 Standardization of Multiple Tempering Cycles. Hardened specimens were subjected to multiple tempering cycles at 450 °C. The hardness profile was used to standardize multiple tempering cycles. Nomenclatures of heat treatment conditions for this experiment are elaborated in Table 2.

The cryogenically treated specimens were subjected to soft tempering to relieve the stresses induced due to thermal shock. Four different soft-tempering temperatures were used: 50 °C, 100 °C, 150 °C, 200 °C (Fig. 2a).

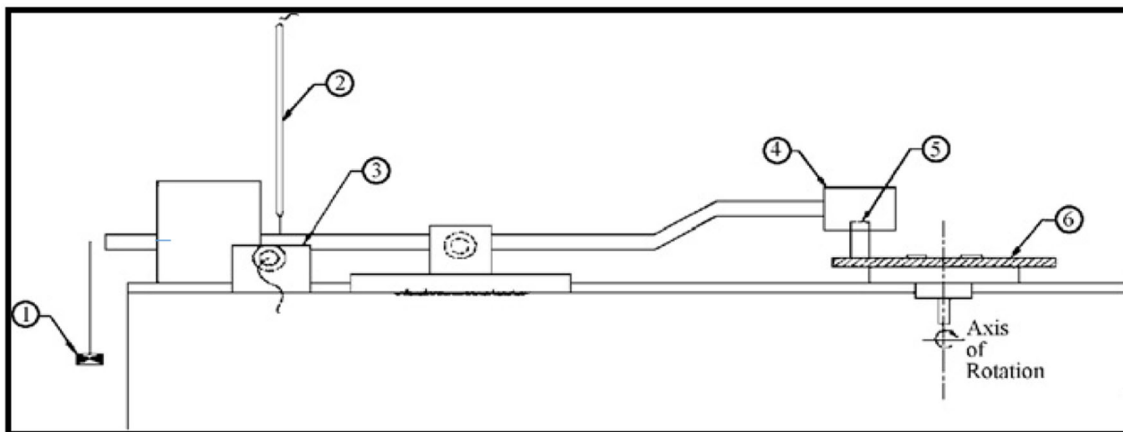
2.3 Material Characterization

2.3.1 Hardness Measurement. Rockwell hardness C-scale tester was used for measurement of hardness. The flat surface was prepared by using SiC-emery paper (600). A minor load of 10 kg was first applied to seat the indenter, followed by major load of 150 kg for 15 s, and resistance to indentation was recorded on the dial gauge. An average of three readings was noted as a measure of hardness.

2.3.2 Wear Testing. The pin-on-disk wear test machine was used to estimate wear loss in dry sliding condition under a specific applied load and sliding speed at room temperature (Fig. 2b) according to ASTM G99. The intension of opting for pin-on-disk setup is to test the material as per the mechanical working conditions. During testing, the pin (i.e., specimen) was kept stationary and the circular disk was kept rotating. The pin



(a)



1. Load, 2.Y-Recorder, 3.Load Cell, 4.Specimen Holder, 5.Specimen, 6. Counterface

(b)

Fig. 2 (a) Processing route for cryogenic treatment, (b) pin-on-disk wear testing machine

Table 2 Nomenclature of heat treatment conditions for standardization of multiple tempering

Treatment notation	Description
H	Hardened and oil quench
HTT	Hardened and double tempered
HTTC8	Hardened, single tempered and cryotreated for 8 h
HTTC8-ST50	Hardened, single tempered and cryotreated for 8 h, soft tempering at 50 °C
HTTC16	Hardened, double tempered and cryotreated for 16 h
HTTC24	Hardened, triple tempered and cryotreated for 24 h

Table 3 Parameters for pin-on-disk wear testing AISI H13

Pin dimensions	Dia. 6 × 10, mm long
Load	3.5, kg
Sliding distance	6000, m
Speed	3, m/s
Track diameter	60, mm

material was AISI H13, and counter-face rotating disk was made of SAE 52100 (C-1.00, Mn-0.35, Si-0.20, S-0.025, P-0.025, Fe-Balance, % by weight) with hardness of 59 HRC. Wear test parameters used in this project work are listed in Table 3. Three specimens were tested to record the average wear loss. Surface roughness measurements indicated an average of 0.55 μm for a set of 15 specimens used in the test.

2.3.3 Metallography. Metallographic techniques were employed for specimen preparation. The sample size for metallographic investigation of AISI H13 was 6 mm in diameter and 10 mm long. The scratches were removed by rough grinding followed by polishing on emery papers (200, 600, 800 and 1200). The final polishing was done on velvet cloth with 0.5 μm diamond paste as an abrasive medium.

A freshly prepared 2% nital solution (nitric acid and ethanol) was used to reveal microstructural constituents through etching. Scanning electron microscope (SEM) (Make: JEOL, Department of Physics, University of Pune) was used for further investigation of microstructures, having a scanning range of 0-20 eV along with EDS analysis. X-ray diffraction analysis was also performed on the conventionally and cryotreated specimens.

3. Results and Discussion

3.1 Hardness Variation in AISI H13

Figure 3 depicts the peak hardness values in conventional treatment and cryogenic treatment, at 500 °C and 450 °C, respectively. Peak hardness has been shifted toward lower temperatures when cryogenic treatment was performed.

The decrease in the hardness was observed when tempering was performed at higher temperatures, which could be attributed to greater driving force required for carbide coarsening at higher temperatures. 10% increase in hardness was reported for cryotreated specimens which could be attributed to transformation of retained austenite into martensite and precipitation of fine carbides. The SEM micrographs of AISI H13 clearly depict the dispersion of fine carbides in the matrix of tempered martensite (Fig. 4a and b). Figure 4(c) and (d) indicates SEM micrograph and EDS analysis of precipitated carbide particles which mainly include Cr_{23}C_6 , MoC and VC type of carbides (Ref 23). Nano-carbides could be detected using TEM images (Ref 23). Figure 4(e) indicates the XRD analysis of conventionally treated and cryotreated specimens. XRD results do not indicate presence of any retained austenite for cryogenically treated specimen thereby confirming the fact that cryogenic treatment helps in conversion of retained austenite into martensite (Ref 23).

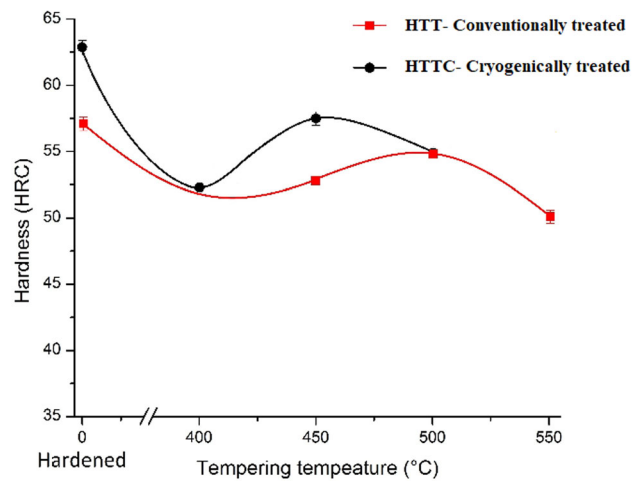


Fig. 3 Effect of tempering temperature on hardness of conventionally and cryogenically treated AISI H13

3.2 Selection of Tempering Cycles

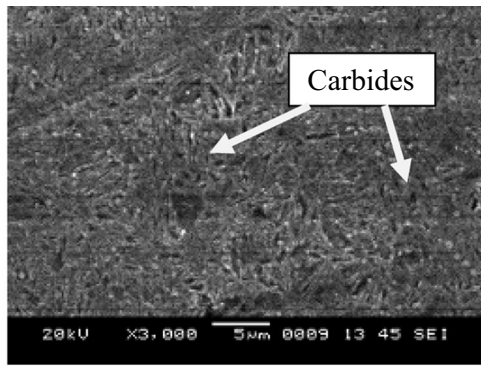
The increased hardness post-cryogenic treatment could be attributed to increased residual stresses as a result of phase transformation of retained austenite to martensite in addition to cold stresses (Ref 8). The soft-tempering post-cryogenic treatment relieved the residual stresses, reduced the retained austenite as well as provided the driving force for the precipitation of fine carbides. For AISI H13, it has been observed that single tempered and double tempered specimens showed small difference in hardness. Considering the generation of residual stresses, double tempering could be preferred.

The hardness decreased when multiple tempering was adopted which could be attributed to softening of martensitic matrix and coarsening of preexisting primary carbides rather than insignificant increase in secondary carbides (Ref 8).

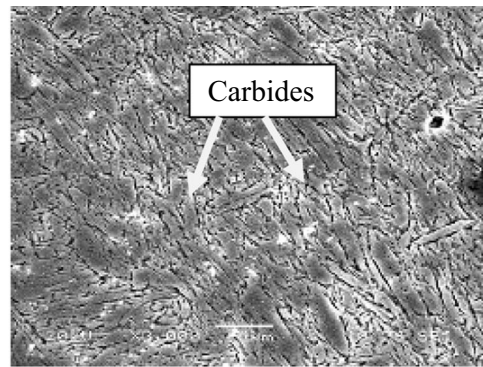
3.3 Wear Mechanism of AISI H13

Figure 5 shows variation of volumetric wear rate with cryosoaking period at various soft-tempering temperatures for AISI H13. Figure 5 shows that cryosoaking period of 24 h clearly divided mild wear regime and severe wear regime.

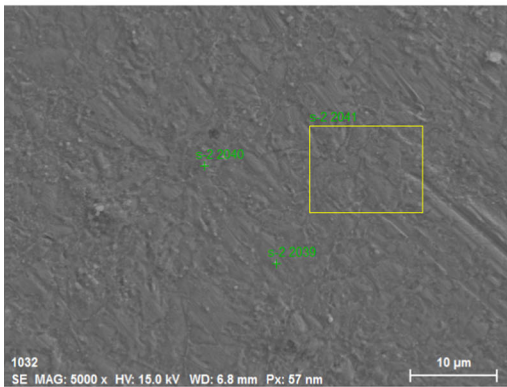
3.3.1 Mild Wear Regime. Mild wear regime corresponds to negative slope of graph in Fig. 5 for the cryosoaking period of 8-24 h. The lowest volumetric wear rate is observed at soft-tempering temperature of 50 °C for the cryosoaking period of 24 h. The worn-out surface of HTTC8-ST50 is shown in Fig. 6(a) indicates ridges along sliding direction which depicts high volumetric wear rate (Fig. 5). The worn-out surface of HTTC16-ST50 in Fig. 6(b) indicates carbide particles in the crack propagation line thus improving the wear resistance to some extent. Also, it indicates mild oxidative wear. The worn-out surface of HTTC24-ST50 in Fig. 6(c) shows deformed layer and crack initiation sites. Figure 5 shows that HTTC24-ST50 has lowest wear rate. This low wear rate could be attributed to greater driving force for tertiary carbide precipitation. These nano-sized carbides played an effective role in increasing wear resistance by increasing the shear strength of matrix (Ref 8). For good wear resistance, cryosoaking period of 24 h and soft-tempering temperature of 50 °C were chosen as standardized parameters.



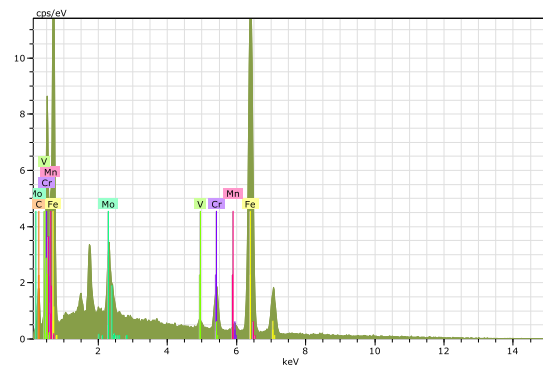
(a)



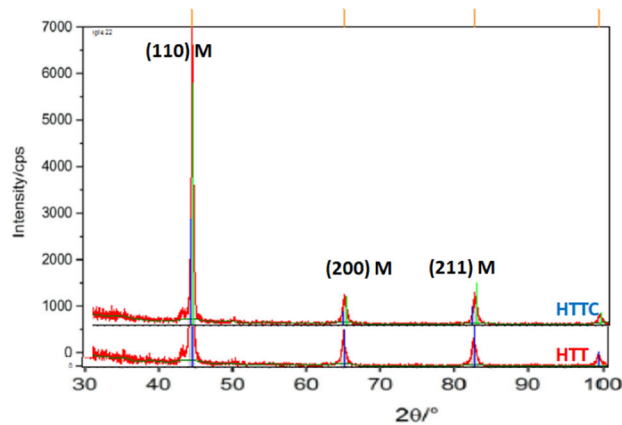
(b)



(c)



(d)



(e)

Fig. 4 (a) SEM micrograph of HTTC8-ST50 of AISI H13 showing carbides dispersed in tempered martensitic matrix [Etched with 2% Nital, $\times 1000$], (b) SEM micrograph of HTTC24-ST50 of AISI H13 showing carbides dispersed in tempered martensitic matrix [Etched with 2% Nital, $\times 1000$], (c) and (d) SEM micrograph and EDS analysis of AISI H13 specimen, (e) XRD analysis of HTT and HTTC Specimens

3.3.2 Severe Wear Regime. The wear rate increased rapidly from cryosoaking period of 24 to 32 h on account of coarsening of carbides at high cryosoaking period (Fig. 5). This positive slope of graph for the cryosoaking period 24-32 h

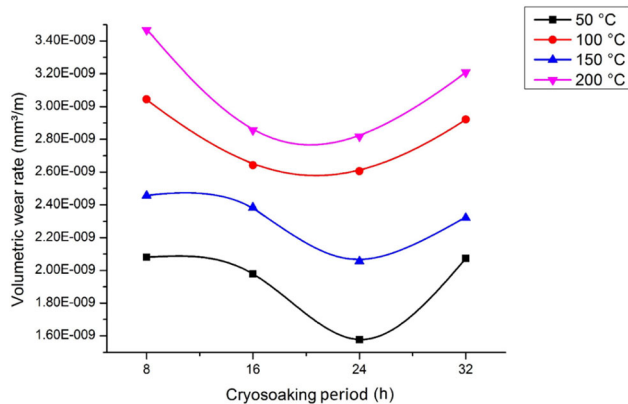


Fig. 5 Effect of cryosoaking period on wear rate of AISI H13 for varying soft-tempering temperature

corresponds to severe wear regime. The worn-out surface of HTTC32-ST50 in Fig. 6(d) shows severely deformed layer with laminated sheets and deformation lips. Also cracking of deformed layer and crack initiation sites were evident. These observations clearly indicated the dominance of severe delamination wear mode.

Figure 7 shows variation of wear rate and hardness with cryosoaking period for AISI H13 for 50 °C soft-tempering temperature. The lowest volumetric loss at 24 h could be attributed to increased tertiary carbide precipitation along with their uniform distribution in cryotreated specimens. HTTC500 indicated high wear rate as compared to cryogenically treated specimens at standardized parameters, i.e., HTTC24-ST50. The decrease in wear rate observed was around 28.53%.

At high cryosoaking period, the wear rate increases rapidly with corresponding decrease in hardness. This might be due to coarsening of preexisting primary carbides and newly precipitated secondary and tertiary carbides at high cryosoaking period.

3.3.3 Standardization of Soft-Tempering Temperature. Figure 8 exhibits the variation of volumetric wear rate with varying soft-tempering temperature for AISI H13 specimens. Soft tempering at high temperature led to the significant

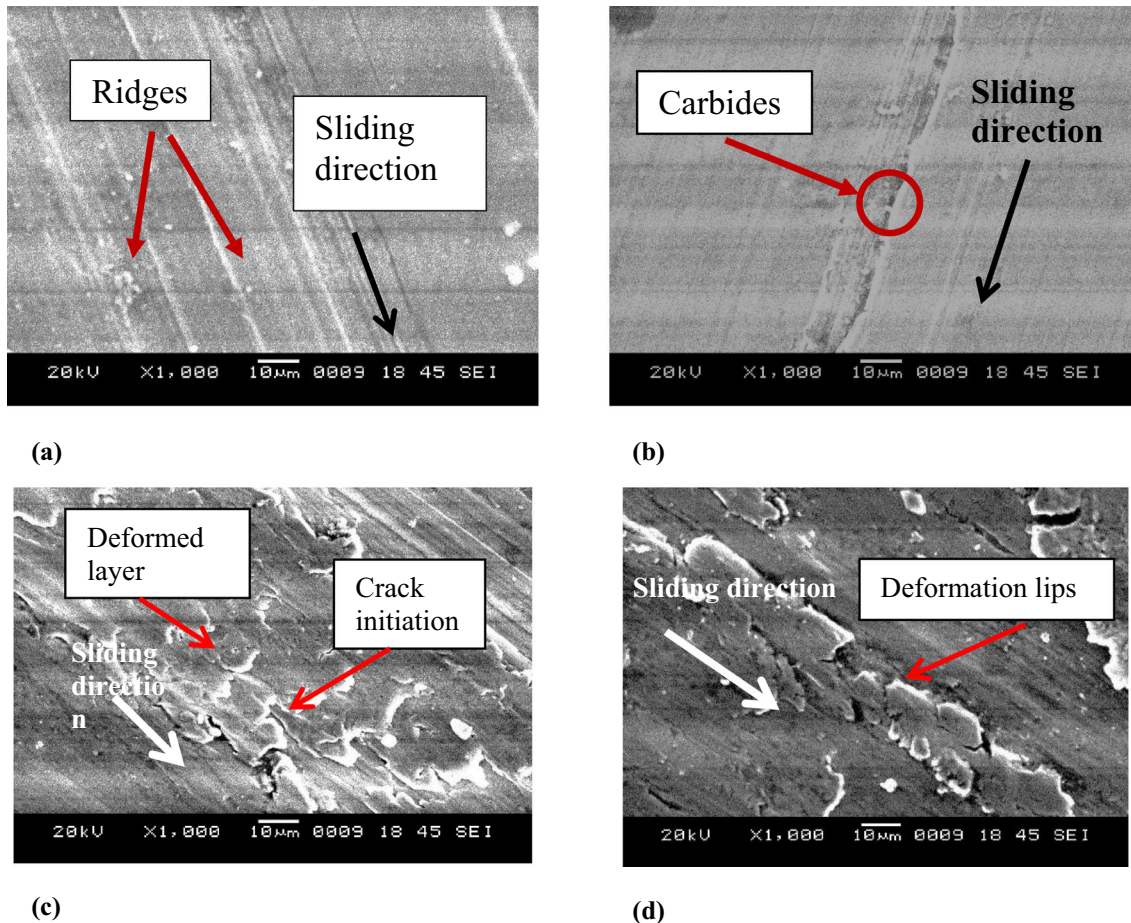


Fig. 6 (a) SEM micrograph of worn-out surface of HTTC8-ST50 of AISI H13 showing dominance of adhesive wear mode, $\times 1000$, (b) SEM micrograph of worn-out surface of HTTC16-ST50 of AISI H13 showing mild oxidative wear with carbides evident along crack propagation line, $\times 1000$, (c) SEM micrograph of worn-out surface of HTTC24-ST50 of AISI H13 showing deformed layer and crack initiation sites, $\times 1000$, (d) SEM micrograph of worn-out surface of HTTC32-ST50 of AISI H13 showing severely deformed layer, laminated sheets, cracks and fractured ridges showing dominance of severe delamination wear mode, $\times 1000$

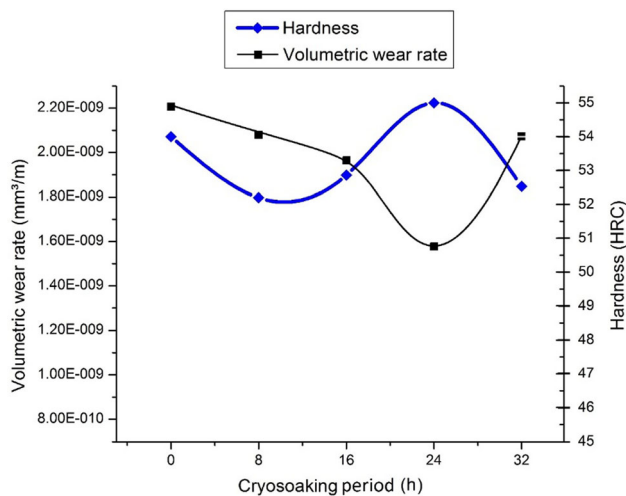


Fig. 7 Effect of cryosoaking period on wear rate and hardness of AISI H13 for 50 °C soft-tempering temperature

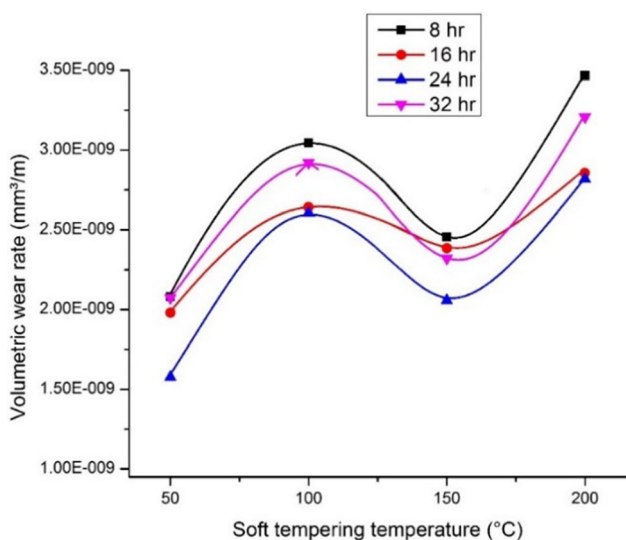


Fig. 8 Effect of soft-tempering temperature on wear rate of AISI H13 for varying cryosoaking period

increase in wear rate. Increase in the size of carbide particles on account of elevated temperature deteriorates mechanical properties (Ref 35). Figure 9 indicates 2D contour plots for AISI H13, which depicts the standardized parameters. These plots could be used to predict wear behavior if cryosoaking period and soft-tempering temperature are known.

Based on the microstructural analysis, EDS and XRD analysis, it could be said that the precipitation of fine tertiary carbides in the matrix of tempered martensite in case of cryogenically treated specimens improved hardness and wear resistance considerably for 24 h of cryosoaking period. AISI H13 specimens have exhibited considerably less roughening of tempered martensitic grains with a finer microstructure on

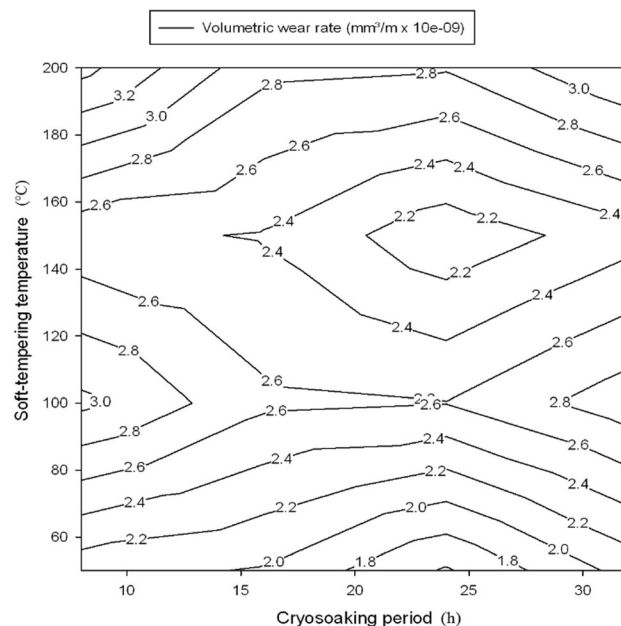


Fig. 9 2D contour plot for effect of cryosoaking period and soft-tempering temperature on volumetric wear rate of AISI H13

account of alloy carbide precipitation which inhibit the grain growth.

4. Conclusion

Following points could be summarized as concluding remarks based upon the analysis and discussion:

- (1) The cryogenic treatment resulted in 10% increase in hardness over conventional treatment. This could be attributed to precipitation of tertiary carbide post-cryogenic treatment and transformation of retained austenite into martensite.
- (2) For multiple tempering treatments, hardness decreased after hardening and cryotreatment which could be attributed to softening of martensitic matrix and coarsening of primary carbides rather than significant increase in secondary carbides. AISI H13 exhibited high hardness on account of higher volume fraction of hard carbides. Hence double tempering was selected as standardized treatment among multiple tempering treatments.
- (3) Soft-tempering temperature was optimized for AISI H13 at 50 °C nearly equivalent to 10% of conventional tempering temperature based on minimum wear rate. Higher soft-tempering temperature could lead to coarsening of carbides due to Ostwald ripening mechanism.
- (4) The decrease in wear rate for cryogenic treatment at standardized parameters as compared to conventionally treated samples was 28.5%, for AISI H13. This drop-in

wear rate could be because of increased hardness by conversion of retained austenite into martensite, precipitation of tertiary carbide during cryogenic treatment.

References

1. ASM International, ASM Handbook for Heat Treating 1991
2. R.A. Mesquita, C.A. Barbosa, E.V. Morales, and H.J. Kestenbach, Effect of silicon on carbide precipitation after tempering of H11 hot work steels, *Metall. Mater. Trans. A*, 2011, **42**, p 461–472.
3. R.A. Mesquita, C.A. Barbosa, and A.R. Machado, Heat Treatment of tool steels, *Comprehensive Materials Finishing*, Vol 2–3, Elsevier, Amsterdam, 2010
4. G.K.G. Roberts, Tool steels, in ASM International 1998
5. P. Jovi, Effectiveness of deep cryogenic treatment on carbide precipitation, *J. Mater. Res. Technol.*, 2020, **9**(6), p 13014–13026.
6. F.H. Çakir and O.N. Çelik, The effects of cryogenic treatment on the toughness and tribological behaviors of eutectoid steel, *J. Mech. Sci. Technol.*, 2017, **31**, p 3233–3239.
7. S. Katoch, R. Sehgal, and V. Singh, Optimization of friction and wear characteristics of varied cryogenically treated hot die steel grade AISI-H13 under dry condition, *Friction*, 2017, **5**(1), p 66–86.
8. T. Shinde and N.B. Dhokey, Influence of tertiary carbides on improving fatigue limit of H13 die steels, *Metallogr. Microstruct. Anal.*, 2017, **6**–5, p 398–406. <https://doi.org/10.1007/s13632-017-0380-7>
9. T. Shinde and N.B. Dhokey, Influence of carbide density on surface roughness and quasi-stable wear behaviour of H13 die steel, *Surf. Eng.*, 2017, **33**(12), p 944–952. <https://doi.org/10.1080/02670844.2017.1312739>
10. D. Senthilkumar and I. Rajendran, A research review on deep cryogenic treatment of steels, *Int. J. Mater. Struct. Int.*, 2014, **8**(1–3), p 169–184. <https://doi.org/10.1504/IJMSI.2014.064784>
11. H.F. Rad, A. Amadeh, and H. Moradi, Wear assessment of plasma nitrided AISI H11 steel, *Mater. Des.*, 2011, **32**(5), p 2635–2643.
12. B. Wang, X. Zhao, W. Li, M. Qin, and J. Gu, Effect of nitrided-layer microstructure control on wear behavior of AISI H13 hot work die steel, *Appl. Surf. Sci.*, 2018, **431**, p 39–43.
13. M. Pellizzari, Influence of deep cryogenic treatment on heat treatment of steel and Cu-Be alloy, *Int. Heat Treat. Surf. Eng.*, 2010, **4**(3), p 105–109.
14. P. Suchmann, D. Jandova, and J. Niznanska, Deep cryogenic treatment of H11 hot working tool steel, *Mater. Techn.*, 2015, **49**, p 400–408.
15. Y. Yao and Y. Zhou, Effects of deep cryogenic treatment on wear resistance and structure of GB 35CrMoV steel, *Metals*, 2018, **8**(7), p 502. <https://doi.org/10.3390/met8070502>
16. P. Jovi and B. Setina, Effect of deep cryogenic treatment on surface chemistry and microstructure of selected high-speed steels, *Appl. Surf. Sci.*, 2021, **548**, p 149–257. <https://doi.org/10.1016/j.apsusc.2021.149257>
17. J. Hidalgo, K.O. Findley, and M.J. Santofimia, Thermal and mechanical stability of retained austenite surrounded by martensite with different degrees of tempering, *Mater. Sci. Eng. A*, 2017, **690**, p 337–347.
18. S. Li, M. Xiao, G. Ye, K. Zhao, and M. Yang, Effects of deep cryogenic treatment on microstructural evolution and alloy phases precipitation of a new low carbon martensitic stainless bearing steel during aging, *Mater. Sci. Eng. A*, 2023, **27**, p 8100–8118.
19. S. Yang, Z. Pu, D.A. Puleo, O.W. Dillon, and I.S. Jawahir, Cryogenic processing of biomaterials for improved surface integrity and product sustainability. In: *Advances in Sustainable Manufacturing: Proceedings of the 8th Global Conference on Sustainable Manufacturing*, 2011, p. 175–176
20. S. Ramesh, B. Bhuvaneshwari, G.S. Palani, D.M. Lal, and N.R. Iyer, Effects on corrosion resistance of rebar subjected to deep cryogenic treatment, *J. Mech. Sci. Technol.*, 2017, **31**(1), p 123–132.
21. A. Günen, İ.H. Karahan, M.S. Karakaş, B. Kurt, Y. Kanca, V.V. Çay, and M. Yıldız, Properties and corrosion resistance of AISI H13 hot-work tool steel with borided B₄C powders, *Metals Mater. Int.*, 2020, **26**, p 1329–1340.
22. Ş. Polat, Ş.H. Atapek, E. Türedi, and G. Aktaş, Wear behaviour of heat treated hot work tool steels under dry sliding conditions, *Mater. Test.*, 2013, **55**(3), p 163–167.
23. S. Li, H. Guo, J. Li, Z. Li, and J. Li, Carbides precipitation and kinetics of H13 steel subjected to deep cryogenic treatment, *Mater. Sci. Technol.*, 2022, **38**(16), p 1376–1389.
24. L. Han, Y. Wang, and S. Liu et al., Effect of cryogenic treatment on the microstructure and mechanical properties of selected laser melted H13 steel, *J. Mater. Res. Technol.*, 2022, **21**, p 5056–5065.
25. A. Çiçek, F. Kara, T. Kivak, E. Ekici, and I. Uygur, Effects of deep cryogenic treatment on the wear resistance and mechanical properties of AISI H13 hot-work tool steel, *J. Mater. Eng. Perform.*, 2015, **24**, p 4431–4439.
26. A. López-Leyva, G. Luis-Pantoja, and J.A. Juárez-Islas et al., Influence of heat and cryogenic treatments on the abrasive wear behavior of H13 tool steel, *J. Mater. Eng. Perform.*, 2023, **32**, p 10254–10264.
27. C.H. Surberg, P. Stratton, and K. Lingenhoe, The effect of some heat treatment parameters on the dimensional stability of AISI, D2, *Cryogenics*, 2008, **48**, p 42–47.
28. P. Baldissera, Fatigue scatter reduction through deep cryogenic treatment on the 18NiCrMo5 carburized steel, *Mater. Des.*, 2009, **30**, p 3636–3642.
29. F. Kara, A. Çiçek, and H. Demir, Multiple regression and ANN models for surface quality of cryogenically-treated AISI 52100 bearing steel, *J. Balkan Tribol. Assoc.*, 2013, **19**(4), p 570–584.
30. K. Amini, S. Nategh, and A. Shafyfi, Influence of different cryotreatments on tribological behavior of 80CrMo12 5 cold work tool steel, *Mater. Des.*, 2010, **31**, p 4666–4675.
31. S. Li, Y. Xie, and X. Wu, Hardness and toughness investigations of deep cryogenic treated cold work die steel, *Cryogenics*, 2010, **50**, p 89–92.
32. A. Çiçek, F. Kara, T. Kivak, and E. Ekici, Evaluation of machinability of hardened and cryo-treated AISI H13 hot work tool steel with ceramic inserts, *Int. J. Refract. Metals Hard Mater.*, 2013, **41**, p 461–469.
33. K. Amini, A. Akhbarizadeh, and S. Javadpour, Investigating the effect of holding duration on the microstructure of 1.2080 tool steel during the deep cryogenic heat treatment, *Vacuum*, 2012, **86**, p 1534–1540.
34. Xu. Jun Li, H.B. Zhang, and H. Qi et al., Effects of deep cryogenic treatment on the microstructure evolution, mechanical and thermal fatigue properties of H13 hot work die steel, *J. Mater. Res. Tech.*, 2023, **27**, p 8100–8118.
35. M. Godec and D.A. Skobir Balantič, Coarsening behaviour of M23C6 carbides in creep-resistant steel exposed to high temperatures, *Sci. Rep.*, 2016, **6**, p 29734.
36. B.A.M. Toprak, A. Çalık, and A. Tekgüler, Effect of boriding on the tribological behavior of Hardox 450 and HiTuf steels, *J. Rev. Adv. Mater. Sci.*, 2020, **59**, p 314–321.
37. B. Aktasa, V. Balaka, and C. Carboga, Dry sliding wear behavior of boron-doped AISI 1020 steels, *Act. Phys. Polo. A*, 2017, **132**, p 455–458.
38. C. Carboga, B. Aktas, and B. Kurt, Dry sliding wear behavior of boron-doped 205 manganese steels, *JMEP*, 2020, **29**, p 3120–3126.

Publisher's Note Springer Nature remains neutral with regard to jurisdictional claims in published maps and institutional affiliations.

Springer Nature or its licensor (e.g. a society or other partner) holds exclusive rights to this article under a publishing agreement with the author(s) or other rightsholder(s); author self-archiving of the accepted manuscript version of this article is solely governed by the terms of such publishing agreement and applicable law.